Sol−Gel-Derived Iron Oxide Thin Films on Silicon: Surface Properties and Interfacial Chemistry

Chi-dong Park,[†] Jeremy Walker,[‡] Rina Tannenbaum,[‡] A. E. Stiegman,*[,†] J. Frydrych,[§] and L. Machala[§]

Department of Chemistry and Biochemistry, Florida State University, Tallahassee, Florida 32306, Department of Materials Science and Engineering, Georgia Institute of Technology, Atlanta, Georgia 30332, and Nanomaterial Research Centre, Palacky University in Olomouc, Svobody 26, 771 46 Olomouc, Czech Republic

ABSTRACT Uniform high-quality iron oxide thin films can be formed from the spin coating of iron oxide/hydroxide sol−gels on a silicon substrate. Thermal processing of the films at temperatures of ∼300 °C results in the transformation of films into a ternary layered structure with iron oxide, Fe_2O_3, at the surface, characterized by Mössbauer spectroscopy, and reduced, metallic iron characterized by depth profiling of the surface by X-ray photoelectron spectroscopy as a function of Ar^+ etching. Imaging of the etched surface by scanning electron microscopy reveals two distinct regions at the interface, nanoparticles that are very iron-rich separated by an unstructured region that is somewhat less iron-rich. The results demonstrate a synthetic protocol for the spontaneous formaton of a ternary layered structure from a simple one-step preparation.

KEYWORDS: interfacial redox reactions • iron oxide thin films • thermite reaction • iron oxide

In a recent report, we have shown that high-quality iron oxide thin films can be formed from the spin coating of iron oxide/hydroxide sol−gels on a silica substrate (1). In this approach, $Fe(H_2O)_6^{3+}$ ions are condensed through the epoxide-catalyzed deprotonation of water in the coordination sphere (2−6). This results in a rapid reaction, which is amenable to thin film formation just prior to gelation. Iron oxide/hydroxide films made in this fashion were converted by an appropriate choice of the thermal processing pathway into good-quality hematite and maghemite thin films.

An interesting aspect of sol−gel-derived metal oxide materials made through epoxide catalysis is that they undergo thermite-type reactions with the incorporation of a fuel (e.g., Al) during gelation. Thermal ignition of the metal/oxide gel composites initiates a self-propagating exothermic redox reaction to produce oxides and reduced metal products (e.g., Fe). We report here an investigation of whether the thin-film-forming properties of the iron oxide/hydroxide gels can be combined with their oxidation−reduction processes to form a layered structure if the film is deposited on a silicon substrate, which can act as a fuel source. From a syntheic standpoint, the ability to spontaneously form a layered structure from a simple one-step preparation can afford some technological advantages. In a typical preparation, 2.59 g of $Fe(NO_3)_3 \cdot 9H_2O$ was added to 10 mL of absolute ethanol. After dissolution, 1 mL of proplyene oxide was added with stirring to 5 mL of the ethanolic Fe^{3+} solution. After 2 min, the solution turned dark and 5 drops were used to spin coat an untreated silicon wafer at 2800 rpm. The product of the propylene oxide catalyzed gelation of $Fe(H_2O)_6^{3+}$ is a largely amorphous iron oxide/hydroxide phase known as ferrihydrite, which also contains organic products of the epoxide catalysis (henceforth referred to as Fe^{3+} gels) (7). As deposited on the silicon wafer using this procedure, the Fe^{3+} gel formed yellow films with a highly uniform appearance (Figure 1a). The film thickness, obtained from profilometry across a scored region of the film, is ∼1 μm. Atomic force microscopy (AFM) in the tapping mode shows the film to be quite flat (Figure 2a) with a surface mean roughness of 0.364 nm. The imaged surface is characterized by small, spikelike features of ∼20 nm diameter.

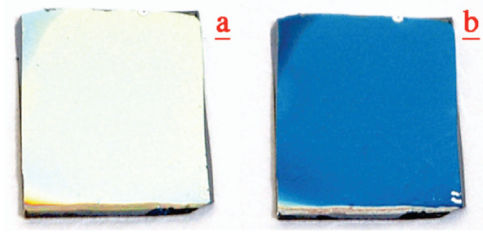

FIGURE 1. Thin films of Fe^{3+} gels spin-coated on a silicon wafer: (a) as deposited; (b) after heating to 300 °C.

Conversion of the gels to an oxide film was accomplished by insertion into a tube furnace at a temperature of 300 °C in air. Heating resulted in an instantaneous transformation of the film from yellow to blue-gray (Figure 1b). The transformation occurs with qualitative retention of the film quality. After heating, the film is about 50% of its original

* E-mail: stiegman@chem.fsu.edu.
Received for review May 27, 2009 and accepted August 02, 2009
[†] Florida State University.
[‡] Georgia Institute of Technology.
[§] Palacky University in Olomouc.
DOI: 10.1021/am900362x

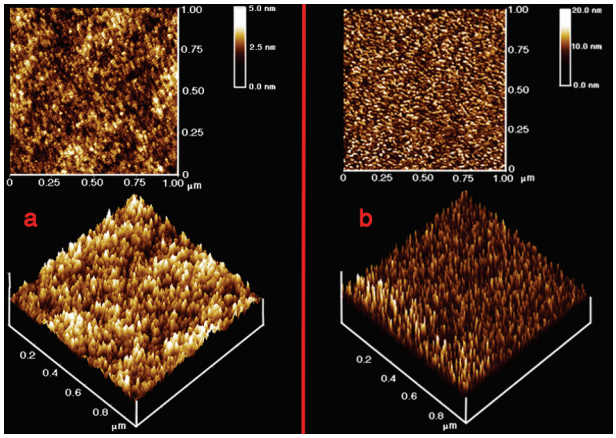

FIGURE 2. AFM image of the surface of (a) as-synthesized and (b) heated (300 °C) Fe^{3+} gel films on silicon.

thickness with a measured value of ~0.5 μm. AFM (Figure 2b), collected in the tapping mode, indicates that the surface of the heated sample is rougher than that of the gel with a root-mean-square roughness of 2.06 nm. The surface shows sharp needlelike features that are narrower than those of the unheated sample.

The thermite reaction between Fe_2O_3 and silicon produces metallic iron and iron(II) silicate, Fe_2SiO_4 (eq 1). As such, we would expect under the best of circumstances to observe completely reduced and partially reduced iron if the reaction goes to completion upon heating (8).

$$4Fe_2O_3 + 3Si \rightarrow 3Fe_2SiO_4 + 2Fe \qquad (1)$$

The identification and characterization of iron-containing phases in both as-synthesized and thermally produced thin films were carried out by use of ^{57}Fe conversion electron Mössbauer spectroscopy (CEMS) and ^{57}Fe conversion X-ray Mössbauer spectroscopy (CXMS). The integral CEMS and CXMS spectra were recorded in a constant acceleration mode using a ^{57}Co radioactive γ-ray source and a proportional continuous-gas-flow counter for room temperature zero-field measurements. A mixture of 90% He (CEMS) or 90% Ar (CXMS) and 10% CH_4 was used as a counting gas. Mössbauer spectra were registered in 1024 channels. The escape (probing) depth of a 7.3 keV K-shell conversion electron is approximately 300 nm, whereas 6.3 keV characteristic Kα conversion X-rays can contain information from a 1−10-μm-thick surface layer of the sample.

CEMS of the as-synthesized sample (Figure 3a) presents one doublet with hyperfine parameters (δ_{Fe} = 0.37 mm/s; ΔE_Q = 0.71 mm/s) typical for (super)paramagnetic iron(III) oxides or hydroxide. Relatively narrow spectral lines ($\Gamma_{1/2}$ = 0.40 mm/s) indicate a narrow distribution of the particle size. No magnetically split component has been detected. Upon CXMS inspection, the whole thickness of the film exhibits practically the same parameters as CXMS. The comparable results from CXMS and CEMS reflect a high degree of homogeneity of the film through the measured thickness. CEMS of the heated sample (Figure 3b) was also evaluated by one doublet (δ_{Fe} = 0.34 mm/s; ΔE_Q = 0.83 mm/s), which

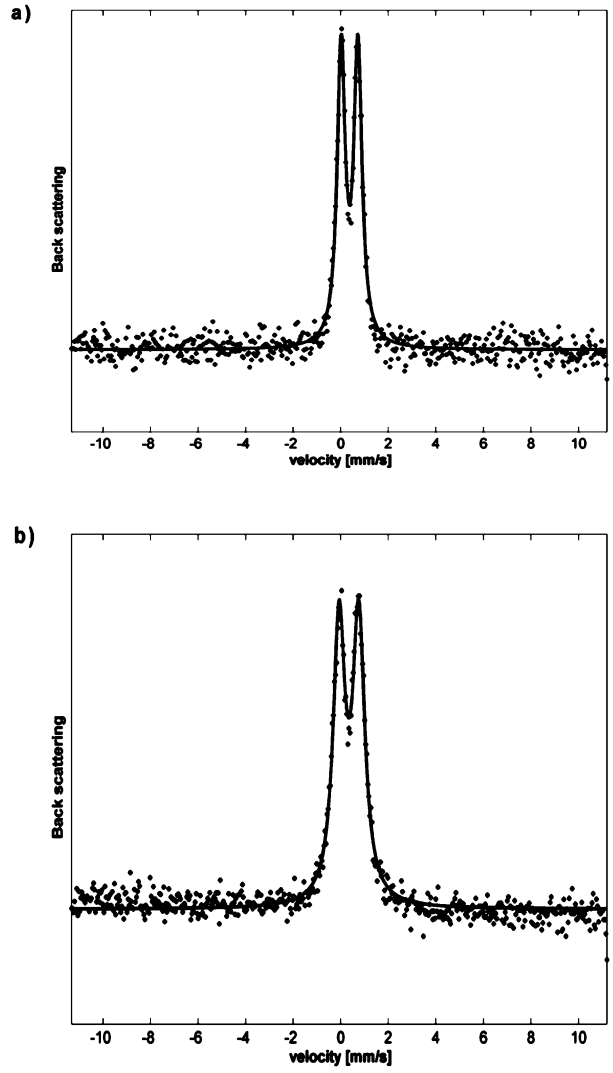

FIGURE 3. CEMS of (a) as-synthesized and (b) heat-treated (300 °C) iron(III) oxide thin films.

can be ascribed to (super)paramagnetic Fe_2O_3; however, the spectral lines are broader ($\Gamma_{1/2}$ = 0.60 mm/s). This can be related to the changes in the particle size and morphology during the heat treatment in accordance with AFM observations. CXMS measured on the heated sample shows a spectrum with almost the same parameters as in the case of CEMS. It is clear from the CEMS and CXMS spectra that the film is an iron oxide similar to what was observed on an inert silica substrate, suggesting that a self-propagating redox reaction that consumes all of the iron film does not occur. This result, however, does not preclude reactivity at the interface, which would be of interest in forming layered structures.

The composition of the thermally produced thin film was analyzed through depth-profiling X-ray photoelectron spectroscopy (XPS) to specifically access the interfacial region between the oxide and silicon. The XPS spectrum (Figure 4) was collected at a 45° takeoff angle from a sample of the heated film on silicon. Consistent with the CXMS and CEMS results, the surface of the film is an iron oxide layer, as indicated by the position of the $2p_{3/2}$ and $2p_{1/2}$ binding energies at 710.3 and 723.8 eV, respectively (9). The film

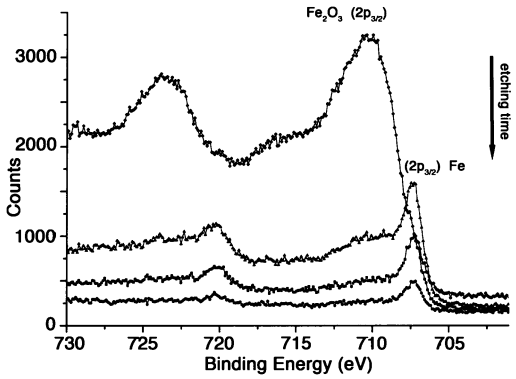

FIGURE 4. XPS of thermally treated (300 °C) Fe^{3+}gel thin films on silicon as a function of Ar^+-ion etching.

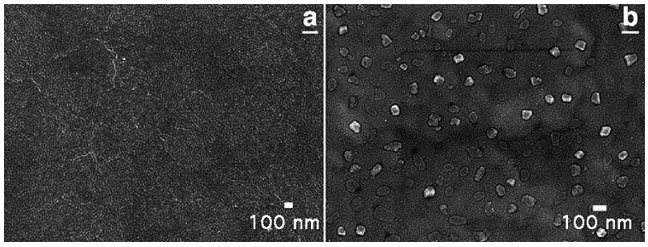

FIGURE 5. Field-emission SEM images of the (a) unetched and (b) Ar^+-ion-etched surface of thermally treated (300 °C) Fe^{3+}oxo/hydroxy thin films.

was etched with an Ar^+-ion gun set at a voltage of 5 keV with an etch rate of ~12 Å/s. As a function of the etching time, the XPS spectrum changes dramatically, with $2p_{3/2}$ ionization narrowing significantly and shifting to 707.3 eV and $2p_{1/2}$ shifting to 720.3 eV (Figure 4). This spectrum is characteristic of metallic iron and indicates that metallic iron has formed below the surface, close to the interface between the Fe^{3+} gel film and the silicon surface. To further verify this result, a control sample of the Fe^{3+} gel was deposited on a non-fuel-fused quartz substrate and heated to form iron oxide, which was depth-profiled under identical conditions (1). This sample showed that, during the course of the etching, only trace amounts of metallic iron were ultimately observed. The formation of these small amounts was consistent with the actions of the Ar^+-ion bombardment, which are sometimes known to generate small amounts of reduced metallic species during etching (10).

Of interest is the nature of the metallic iron that forms at the interface, some characteristics of which are observable in images obtained from scanning electron microscopy (SEM). The field-emission SEM image of a heated film surface (Figure 5a) shows it to be relatively uniform, with some cracking observable in the image. The morphology observed in the SEM compares qualitatively to the Fe_2O_3 films obtained from the heating of thin films of the Fe^{3+}oxo/hydroxy gels deposited on silica. The dimensions of these features on silica were on the order of ~200 nm, while the films formed on the silicon wafer were significantly smaller (<100 nm across) (1). While the origin of this difference is not completely clear, it probably reflects a difference in the film-forming properties of the substrate (surface roughness, hydrophobicity, etc.) or a difference in the heating time and temperature (the films on silica were heated at 600 °C for 6 h). Imaging of the Ar^+-ion-etched region of the sample is shown in Figure 5b. Clearly observable in this image are irregular particles whose lengths are on the order of 50−100 nm residing on what appears to be an amorphous background. Close imaging of the particles does not show any direct evidence of crystallinity such as crystal faces, suggestive of crystallite formation. Attempts to obtain X-ray diffraction data were not successful because of the low concentration of the iron and the dominance of the silicon diffraction. As such, while the particles do not appear to be crystalline, that cannot be ruled out completely.

The elemental composition of the various regions was measured using X-ray dispersion spectroscopy collected from a 5−10 nm spot, which was able to analyze a specific particle. The elemental composition of the unetched surface of a heated sample is, as expected, dominated by silicon, with large contributions from the gold/palladium coating applied for imaging. Iron and oxygen are observed in approximately a 1:3 mole ratio, consistent with the Fe_2O_3 surface detected by CXMS, CEMS, and XPS. The excess oxygen likely arises from the SiO_2 present on the silicon. Imaging of the etched region shows a sharp decrease in the amount of oxygen present relative to the amount of iron, consistent with reduced iron species, particularly the metallic iron detected by XPS. The composition measured in the region between the particles and of the individual particles themselves gave Fe/O mole ratios of 1.3:1 and 2.0:1, respectively. This suggests that the nanoparticles are indeed richer in iron that forms at the interface during thermal treatment. The oxygen present in the etched region at the interface has several probable origins, one is from the iron silicate product, Fe_2SiO_4, and SiO_2 that is already present on the surface. These particles appear dispersed in a medium that also contains reduced iron (possibly amorphous).

Clearly, a key aspect of this interfacial reaction is that it is not a self-propagating high-temperature reaction such as has been used to produce granular $Fe-Al_2O_3$ films from aluminum and iron oxide bi- and multilayers (11−13). In this system, reduced iron is produced only at the interface and at a temperature well below what is required to initiate the combustion of bulk thermite. In fact, attempts to initiate a self-propagating reaction using higher temperatures were not successful. The size and distribution of the reduced iron particles at the interface and the low temperatures at which they form may be due to the thickness and irregularities of the native oxide layer on the silicon surface. The native oxide layer growth in air at room temperature is typically 20 Å, depending on the silicon surface and the specific conditions of oxidation; moreover, the surface is rough with variation in the thickness observed by techniques such scanning force microscopy (14−16). The reduced iron particles may well form in the thinner regions, which affords more intimate contact and lowers the activation barrier to electron- and oxygen-atom-transfer processes.

Acknowledgment. This work has been supported by the Projects of the Ministry of Education of the Czech Republic (Projects MSM6198959218 and 1M619895201) and the

Academy of Sciences of the Czech Republic (Project KAN115600801).

REFERENCES AND NOTES

(1) Park, C. D.; Magana, D.; Stiegman, A. E. *Chem. Mater.* **2007**, *19*, 677.
(2) Clapsaddle, B. J.; Gash, A. E.; Satcher, J. H.; Simpson, R. L. *J. Non-Cryst. Solids* **2003**, *331*, 190.
(3) Clapsaddle, B. J.; Sprehn, D. W.; Gash, A. E.; Satcher, J. H.; Simpson, R. L. *J. Non-Cryst. Solids* **2004**, *350*, 173.
(4) Gash, A. E.; Tillotson, T. M.; Satcher, J. H.; Hrubesh, L. W.; Simpson, R. L. *J. Non-Cryst. Solids* **2001**, *285*, 22.
(5) Gash, A. E.; Tillotson, T. M.; Satcher, J. H.; Poco, J. F.; Hrubesh, L. W.; Simpson, R. L. *Chem. Mater.* **2001**, *13*, 999.
(6) Tillotson, T. M.; Gash, A. E.; Simpson, R. L.; Hrubesh, L. W.; Satcher, J. H.; Poco, J. F. *J. Non-Cryst. Solids* **2001**, *285*, 338.
(7) Gash, A. E.; Satcher, J. H.; Simpson, R. L. *Chem. Mater.* **2003**, *15*, 3268.
(8) Spector, M. L.; Suriani, E.; Stukenbr., G. *Ind. Eng. Chem. Process Des. Dev.* **1968**, *7*, 117.
(9) Mills, P.; Sullivan, J. L. *J. Phys. D: Appl. Phys.* **1983**, *16*, 723.
(10) Asami, K.; Desa, M. S.; Ashworth, V. *Corros. Sci.* **1986**, *26*, 15.
(11) Miagkov, V. G.; Polyakova, K. P.; Bondarenko, G. N.; Polyakov, V. V. *J. Magn. Magn. Mater.* **2003**, *258*, 358.
(12) Myagkov, V. G.; Bykova, L. E.; Li, L. A.; Turpanov, I. A.; Bondarenko, G. N. *Dokl. Phys.* **2002**, *47*, 95.
(13) Myagkov, V. G.; Polyakova, K. P.; Bondarenko, G. N.; Polyakov, V. V. *Phys. Solid State* **2003**, *45*, 138.
(14) Hosaka, S.; Koyanagi, H.; Hasegawa, T.; Hosoki, S.; Hiraiwa, A. *J. Appl. Phys.* **1992**, *72*, 688.
(15) Morita, M.; Ohmi, T.; Hasegawa, E.; Kawakami, M.; Ohwada, M. *J. Appl. Phys.* **1990**, *68*, 1272.
(16) Philipp, H. R.; Taft, E. A. *J. Appl. Phys.* **1982**, *53*, 5224.

AM900362X